Topographic organization of human visual areas in the absence of input from primary cortex *

Heidi A. Baseler[1] Antony B. Morland[1,2]
Brian A. Wandell[1]
[1] Psychology Dept. and Neurosciences Program
Stanford University, Stanford, CA 94305
[2] Biophysics Section, Physics Department, Imperial College, London, UK

January 12, 1999

Preprint - Please do not distribute

Running Head: Visual area topography without primary cortical input.

Keywords: fMRI, retinotopy, visual areas, cortical plasticity, V1, hemianope

Pages: 35; **Figures:** 10; **Tables:** 0

Word Count: 190 (Abstract), 580 (Introduction), 1400 (Discussion)

Correspondence:
Heidi Baseler
Department of Psychology, Jordan Hall, Bldg. 420
Stanford University, Stanford, CA 94305
telephone: (650) 725-1255; FAX: (650) 723-0993;
email: heidi@white.stanford.edu

Abstract

Recently, there has been evidence for considerable plasticity in primary sensory areas of adult cortex. In this study, we asked to what extent

*We thank G. Boynton, J. Demb, N. Sobel for comments on the manuscript. We thank R. Taylor and T. Aron for developing the gray matter segmentation and rendering software and S. Chial for her work on cortical unfolding. Supported by NIH / NRSA, the Wellcome Trust and the McKnight Foundation.

topographical maps in human extrastriate areas reorganize following damage to a portion of primary visual (striate) cortex, V1. Functional magnetic resonance imaging (fMRI) signals were measured in a subject (G.Y.) with a large calcarine lesion that includes most of primary visual cortex (V1) but spares the foveal representation. When foveal stimulation was present, intact cortex in the lesioned occipital lobe exhibited conventional retinotopic organization. Several visual areas could be identified (V1, V2, V3, V3a and V4v). However, when stimuli were restricted to the blind portion of the visual field, responses were found mainly in dorsal extrastriate areas. Furthermore, cortex that had formerly shown normal topography now represented only the visual field around the lower vertical meridian. Several possible sources for this reorganized activity are considered, including transcallosal connections, direct subcortical projections to extrastriate cortex, and residual inputs from V1 near the margin of the lesion. A scheme is described to explain how the reorganized signals could occur based on changes in the local neural connections.

Introduction

A general view of brain development holds that some aspects of neural development arise without the benefit of experience while others will depend on sensory experience. Within the visual pathways, for example, it has been suggested that the eye-specific domains and perhaps topographic organization within the lateral geniculate nucleus (*LGN*) and its recipient cortical areas arise early in development without the benefit of visual experience (Shatz, 1996). Hubel and Wiesel (1970) described experience dependent reorganization of eye-specific domains in LGN and primary visual cortex during a “critical period” early in development.

Recently there has been strong evidence for considerable plasticity in primary sensory areas of adult cortex. For example, topographical remapping of sensory space can occur after primary inputs are removed, or even in undamaged brains after learning (Buonomano & Merzenich, 1998). Receptive fields in primary visual cortex appear to vary in response to changes in recent stimulus history (Kaas et al., 1990; Heinen & Skavenski, 1991; Gilbert & Wiesel, 1992; Gilbert, 1998).

In this study, we ask to what extent topographical maps in human extrastriate areas reorganize following damage to a portion of primary visual (striate) cortex, V1. While alternate pathways exist from retina and LGN to extrastriate cortex, their inputs are relatively sparse (Yukie & Iwai, 1981; Fries, 1981; Standage & Benevento, 1983; Bullier & Kennedy, 1983; Kaas & Huerta, 1988). Thus, destruction of V1 eliminates the main source of visual signals delivered to extrastriate cortical areas and presents an opportunity for considerable reorganization.

We consider three possible consequences of a partial V1 lesion on the responses in extrastriate areas. First, it is possible that extrastriate cortex will be unable to reorganize after the critical period. In this case, large extrastriate regions will remain silent following damage to a portion of V1. Second, it is possible that despite the removal of the V1 signal, intact regions of extrastriate cortex will retain normal topographic representation based on signals received from alternate subcortical or transcallosal inputs. Third, it is possible that extrastriate cortex has reorganized, and can recruit inputs from the spared portion of V1.

We investigated the topographic organization of cortical signals in G.Y., an individual with a large lesion in left anterior calcarine cortex. Based on structural brain images and behavioral testing, the lesion appears to include the peripheral representation of V1, but not the occipital pole, sparing G.Y.'s foveal representation. G.Y. has been studied in a variety of behavioral and neuroimaging experiments, so that much is known about his visual abilities (e.g., Barbur et al., 1980ab; Blythe et al., 1987; Barbur et al., 1993). A previous study, using positron emission tomography (PET), demonstrated extrastriate activity in G.Y. when moving stimuli were presented to the blind portion of his visual field (Barbur et al., 1993). However, functional area mapping was not done and the identity of the active regions were estimated using anatomical landmarks.

Using functional magnetic resonance imaging (fMRI), we measured visual responses in G.Y.'s occipital lobes to determine the topography in spared regions of cortex. When visual stimulation included the spared foveal region, the intact portion of G.Y.'s lesioned occipital lobe exhibited conventional topographical organization. Several retinotopically organized visual areas could be identified. However, when stimuli were confined to the blind portion of his visual field, activity was restricted to dorsal extrastriate areas. Furthermore, these areas exhibited abnormal retinotopic organization. Thus, the same region of cortex appeared to be driven by topographically different inputs depending on the stimulus. The measurements suggest that human extrastriate cortex maintains some topographical plasticity after cortical lesions.

Methods

Subjects

Subject G.Y., age 41, sustained damage to the posterior part of his brain in a road accident at age 8. Structural magnetic resonance images reveal two lesions. One lesion falls on the medial aspect of the left occipital lobe, slightly anterior to the

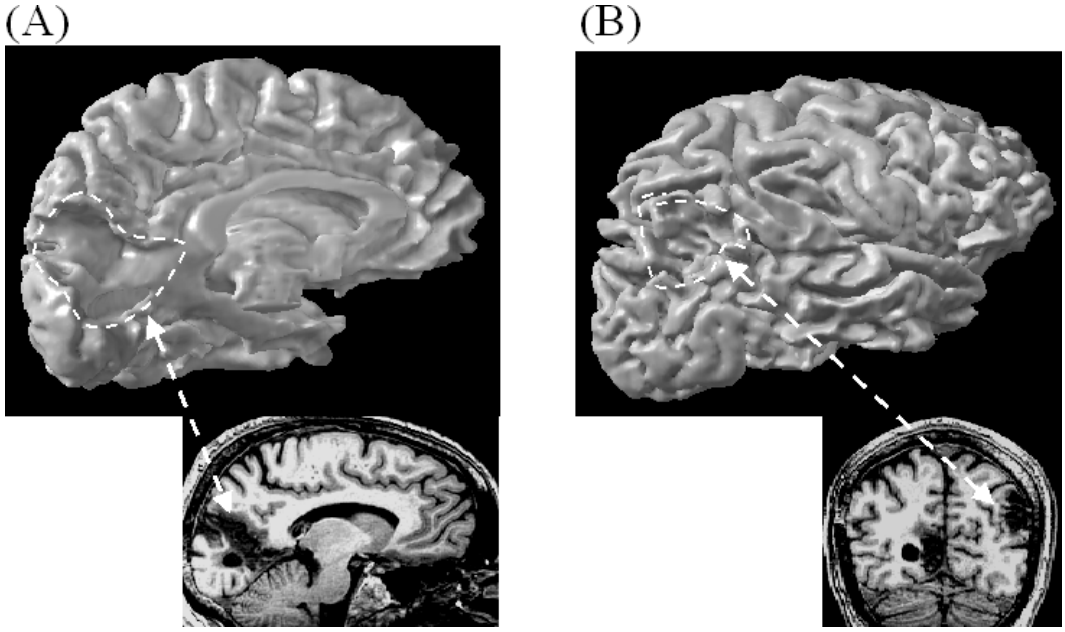

Figure 1: Two lesions in G.Y.'s brain. Upper images contain a three dimensional rendering of the cortical surface near the boundary between gray and white matter, obtain from structural MR data. Lower images contain single slices from structural data. (A) Medial aspect of G.Y.'s left hemisphere. A large lesion is visible near the location ordinarily occupied by calcarine cortex (dashed curve). The sagittal slice below shows the same lesion. (B) Lateral aspect of G.Y.'s right hemisphere, showing the smaller, right parietal lesion (dashed curve), with a corresponding coronal image.

spared occipital pole (Figure 1A). The lesion extends dorsally to the cuneus and ventrally to the lingual, but not fusiform gyrus. The second lesion falls mainly in the inferior parietal lobule and supramarginal gyrus of the right parietal lobe (Figure 1B. Although the parietal lesion is smaller than the occipital lesion, it was the site of the structural damage caused by the road accident.

Based on tests of visual perimetry, G.Y. appears blind within the right visual field at nearly all eccentricities beyond 2.5 deg (homonymous hemianopia with macular sparing) (Barbur et al., 1980a,b; Blythe et al., 1987; Barbur et al., 1993; Kentridge et al., 1997). The results of the most recent visual field measurements of G.Y. are shown in Figure 2 (from Barbur et al., 1993). Within his blind visual field, however, G.Y. retains a range of residual visual capacities, though all aspects of his vision are significantly impoverished compared to normals. His residual vision includes some ability to discriminate color (Brent et al., 1994) and orientation (Morland et al., 1996). G.Y. is particularly sensitive to visual motion and transient stimuli (Barbur et al., 1980a,b; 1993). Residual vision to motion has been reported in other cases of cortical blindness (Blythe et al., 1987; Celesia et al., 1991; Perenin, 1991).

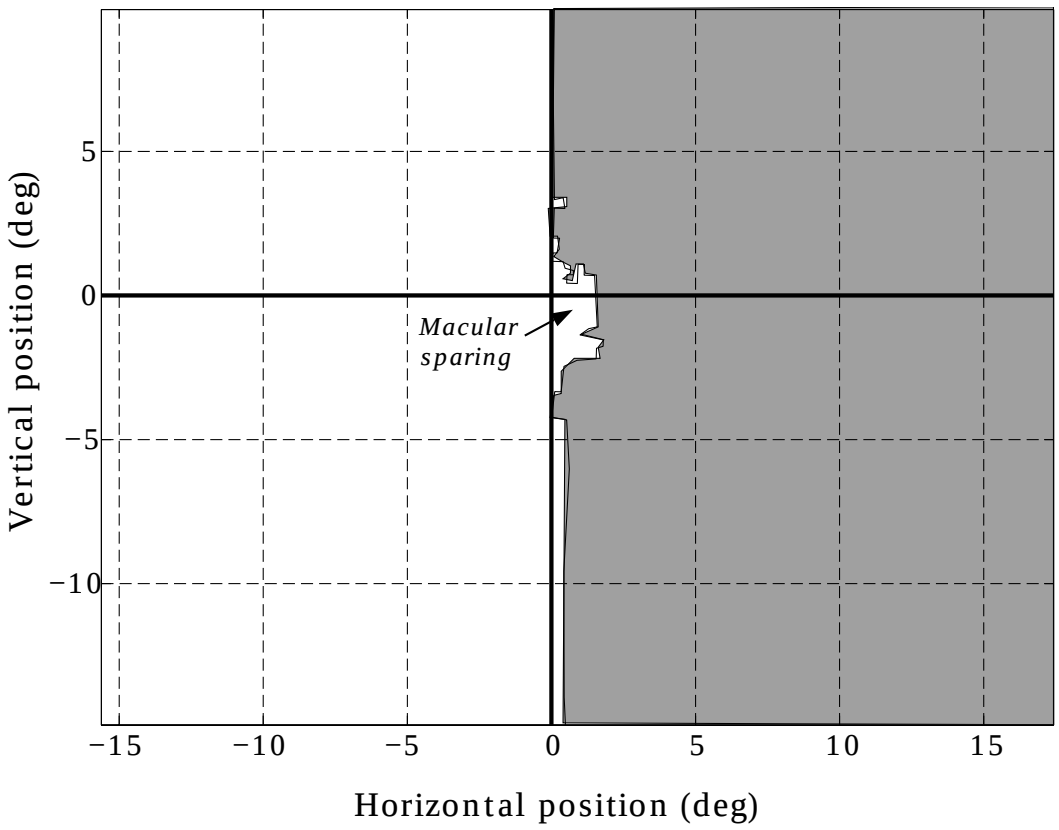

Figure 2: Measurement of G.Y.'s visual field sensitivity, using specialized visual perimetry. White area indicates normal sensitivity; gray area indicates region of visual field loss. (Modified from Barbur et al., 1993.)

Visual behavioral responses to stimuli in G.Y.'s left hemifield are normal, despite the right parietal lesion. His right occipital lobe appears to have suffered no damage in structural MRI records. Therefore, we used responses measured in his right occipital lobe as a control to compare with those measured in his lesioned, left occipital lobe. Subject A.P., who has no known lesions also served as a control.

Both subjects were highly experienced at tasks requiring good visual fixation. Previous studies have shown that G.Y. can fixate reliably, at least for short periods: 20-40 minutes of arc over several seconds (Barbur et al., 1993; Weiskrantz et al., 1995; Kentridge et al., 1997). A recent study confirmed that experienced observers can also fixate quite accurately over extended periods such as those used in neuroimaging experiments (Lucas et al., 1996).

Data acquisition

Magnetic resonance images were acquired using a 1.5 T GE Signa scanner and special purpose head coil or a surface coil placed at the back of the head. Images were collected in 8 planes oriented either perpendicular or parallel to the calcarine sulcus. Eight functional images, measuring a blood oxygenation level dependent (BOLD) signal (Ogawa et al., 1990), were acquired every 3 sec using a 2-shot, 2D spiral gradient-recalled echo sequence (Meyer et al., 1992; Glover and Lai, 1998; TE / TR / FA = 40ms / 1500ms / 90deg; voxel size: 1 x 1 x 4 mm; effective spatial resolution: 1.5 x 1.5 x 4 mm). Structural (T1-weighted) images were acquired in the same planes and resolution as the functional images in order to co-register the functional and anatomical data.

Retinotopic mapping

Human primary visual cortex and several other nearby visual areas are retinotopically organized. To locate and identify early visual areas in occipital cortex, we used a mapping procedure that takes advantage of the retinotopic organization of these areas (Engel et al., 1994, 1997; Sereno et al., 1995; DeYoe et al., 1996).

A slowly expanding annulus was used to map the *eccentric* representation. The annulus was comprised of a black and white checkerboard contrast pattern presented on a gray background (Figure 3B, inset). The checkerboard contrast pattern flickered at 7.4 Hz. Subjects fixated while the annulus expanded from the central fixation point to either 8 or 13 deg of eccentricity once every 36 sec. Check size varied slightly with eccentricity; checks were about 1 degree of visual angle in the eccentric dimension, and ranged from 0.3 to 2.1 degrees of visual angle (15

degrees of polar angle) in the angular dimension. The annulus traveled from fixation to periphery 7 times during each scan (total time = 7x36 = 252 sec). Data from the first cycle were discarded to avoid early transients in the fMRI signal. Brain regions processing a particular position in the visual field were activated when the reversing check pattern passed through that position.

A rotating wedge (Figure 3A, inset) was used to map *angular* position in the visual field. The checkerboard pattern inside the 90 deg wedge reversed at 6.66 Hz. Other temporal parameters (rotation rate, number of cycles, etc.) were similar to those used to map eccentricity. Several retinotopically organized visual areas (V1, V2, V3 and V3a) in the normal human brain abut one another at the vertical and horizontal meridian representations. Boundaries between these areas can be identified from the positions of the horizontal and vertical meridians measured using the rotating wedge stimulus.

In both G.Y. and a normal control, measurements were made using two different rotating wedge patterns. In the *full wedge* condition the stimulus spanned a radius of 8 deg of visual angle. In the *annular wedge* condition the wedge was confined to the blind region of his right visual field, spanning only the eccentricities between 4 and 8 deg from the fovea (Figure 3C, inset). Our strategy was to identify visual area boundaries using the full wedge stimulus and then compare the activity caused by stimulation within the blind visual field. In this way we could compare the activity driven primarily by the LGN to V1 pathways (full wedge) with activity driven by the secondary spared visual pathways (annular wedge).

Data analysis

The *correlation* and *phase* of the fMRI signal were measured using the methods described in Engel et al. (1997). Briefly, the Fourier transform of the fMRI signal time series was calculated for each voxel of the functional images. The amplitude and phase of the time series harmonic at the fundamental stimulus frequency were measured. The correlation was calculated as the square root of the ratio of the squared amplitude of the response at the stimulus frequency divided by the sum of the squared amplitudes at all frequencies.

The phase of the fMRI signal can be used to identify the angular (or eccentric) position of the stimulus causing the response. To relate the response phase of the fMRI signal to the stimulus position, it is necessary to account for the response delay inherent in the hemodynamics, a delay on the order of 4-6 secs (Boynton et al., 1996). The stimulus alternation at a given point in the visual field is a temporal squarewave with a 25 percent duty cycle. The phase of the squarewave fundamental is advanced

approximately $\pi/4$ radians, corresponding to roughly 4.5 sec for a period of 36 sec. Because the phase advance of the stimulus fundamental compensates for hemodynamic delay, the phase of the fMRI signal can be used without modification to estimate the stimulus position.

Cortical unfolding

We computationally unfolded the occipital cortex of each observer in order to visualize functional activity across the cortical sheet and to identify the retinotopic visual areas (Engel et al., 1997; http://white.stanford.edu). Flattening was performed based on high resolution structural 3D volumes measured in each subject's brain (voxel size: 0.9 x 0.9 x 1.2 mm). Gray matter was segmented (Teo et al., 1997) within the images and then unfolded into a 2-dimensional representation of the cortical surface. Functional data were aligned to the high resolution volumes and projected onto the flattened gray matter, creating 2-dimensional phase and correlation maps.

The data shown in all figures were spatially blurred by convolution with a Gaussian kernel to improve the signal-to-noise of the measurements. The Gaussian kernel had a standard deviation of 1.4 mm (support of 10 x 10 mm). The spatial averaging takes place along the cortical surface and thus only includes measurements that arise within the cerebral cortex. By averaging within the flattened representation, signals outside the gray matter are suppressed.

Results

Retinotopic organization within occipital cortex

The retinotopic organization and arrangement of several visual areas in the left occipital lobe of a normal control are shown in Figure 3. Each panel represents the data acquired from eight parallel planes in the left occipital lobe. The data from the separate planes were integrated into a single image by computationally unfolding the gray matter and superimposing the measured fMRI signal onto the flattened representation of cortex.

The color in the figure denotes the location within the visual field of the stimulus that caused the activity. The association between the representation of the visual field and color are shown by the colored legends near each panel; the gray icons indicate the stimulus type. The colored regions show activity levels where the

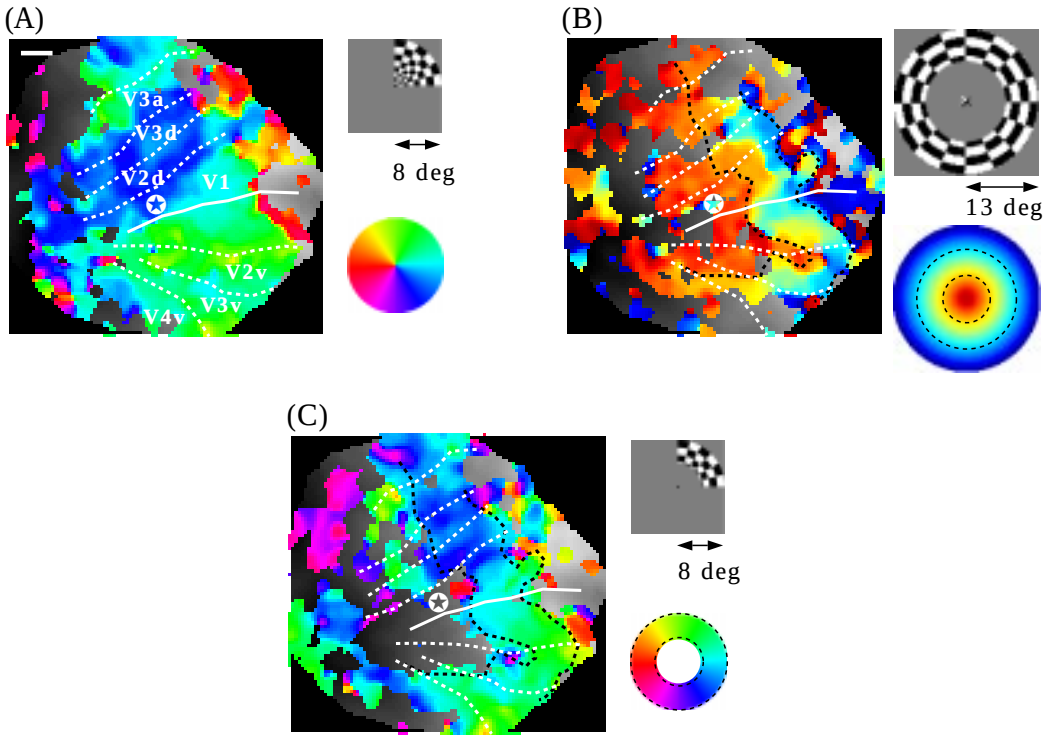

Figure 3: Representations of a control (AP) subject's unfolded left occipital cortex. The underlying gray scale image, which is mainly obscured by the overlaid activity, represents the unfolded cortex. Dorsal / ventral = up / down, and posterior / anterior = left / right on all images in this and the following figure. The gray scale represents the lateral / medial dimension; dark pixels originate from lateral parts in the 3d folded cortex are and light pixels from medial parts. The white scale bar in the upper left corner represents 1 cm. Anatomical landmarks are indicated by the star (occipital pole) and the solid white line (fundus of the calcarine sulcus). The color overlay in each image represents the stimulus position that caused activity at each point in cortex. Color overlays are shown only at positions above the estimated noise level, a correlation of 0.2. The icons to the right of each panel indicate the stimulus type (upper icon) and the relationship between color and visual field position (lower icon). Rotating wedge stimuli spanned an 8 deg radius; expanding ring stimuli spanned a 13 deg radius. Visual area boundaries are represented by white dashed lines drawn by hand along the horizontal and vertical meridians; areas are labeled in the first panel. Black dashed lines represent 4 and 8 deg eccentricity (the extent of the annular wedge), drawn based on the eccentricity map in panel B. (A) Representation of polar angle mapped by the rotating full wedge stimulus. (B) Representation of visual field eccentricity mapped by the expanding ring stimulus. (C) Representation of polar angle mapped by the rotating annular wedge stimulus.

correlation between the response and stimulus fundamental frequency exceeded 0.20. For all thresholds above this level, the images are consistent with the one shown. Below this correlation level the images appear noisy and the spatial pattern of angular positions takes on a patchy, random appearance.

The patchiness near the foveal representation in the eccentricity map in Figure 3 may have been a result of the reduced resolution parallel to the calcarine. In the control subject, slices were oriented perpendicular to the calcarine sulcus to optimize resolution for mapping polar angle and visual area identification. In G.Y., however, eccentricity and polar angle were mapped in separate scanning sessions. Slices were oriented parallel to the calcarine when mapping eccentricity and perpendicular to the calcarine when mapping polar angle.

The retinotopic organization of G.Y.'s intact, right occipital lobe (not shown here) was similar to that of the normal, A.P., and to other measurements in our lab and by others using similar methods (e.g., Engel et al., 1997; Smith, et al., 1998).

Figure 4 shows the retinotopic mapping in the unfolded, left, lesioned occipital lobe in G.Y. Figure 4A shows responses to the full wedge. There is a great deal of spatially organized activity, with the upper quarter field represented in the ventral aspects and the lower quarter field represented in the dorsal aspects. Boundaries between several areas are plainly visible where the angular representation reverses direction. This stimulus reveals that the residual cortex in the lesioned occipital lobe has a conventional retinotopic organization, and includes dorsal and ventral areas V2 and V3. Portions of V3a and V4v can also be seen. Activity in the spared portion of V1 is less extensive and somewhat more disorganized than in the normal (Figure 3A). However, it is not certain whether this difference is significant or whether it is due to partial volume effects by the relatively large functional voxels spanning the narrow calcarine sulcus.

Figure 4B shows responses to the expanding ring stimulus. The activity is consistent with the macular sparing evident in G.Y.'s visual perimetry maps: most of the activity represents eccentricities less than 2.5 degrees. Beyond this eccentricity, activity is patchy or absent.

Figure 4C shows responses to the annular wedge stimulus. The annular wedge fell in the periphery, beyond the macular sparing in the right hemifield. The responses are more fragmented than they were to the full wedge, and the reduction is particularly striking in area V1. The upper visual field representations in V2v, V3v and V4v show relatively little activity. However, there is significant activity particularly in the lower visual field representations of V2d, V3d and V3a in the region beyond the 2.5 deg iso-eccentricity contour marking G.Y.'s macular sparing. The flat map of G.Y.'s lesioned occipital lobe reveals that the lesion has removed

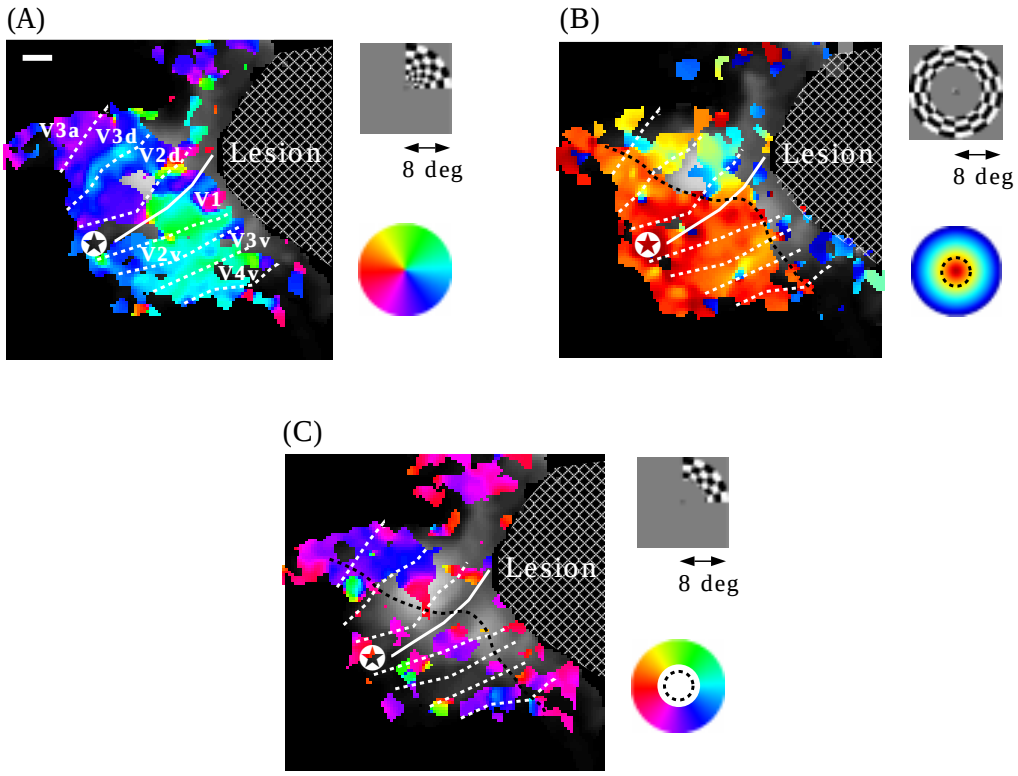

Figure 4: Retinotopic organization of the unfolded left (damaged) occipital cortex of subject G.Y. The position of the lesion (hatched area) was determined by hand-marking the lesion boundaries in the structural MR image slices and transforming them to coordinates in the unfolded representation. The black dashed line marks the 2.5 deg iso-eccentricity contour based on the eccentricity map in (B). It represents the outer boundary of G.Y.'s spared central vision (Figure 2). Other details are as in Figure 3. (A) Representation of the angular dimension mapped by the full rotating wedge stimulus. (B) Representation of the eccentric dimension measured using an expanding ring stimulus. (C) Representation of the angular dimension mapped with the annular rotating wedge stimulus.

more of the peripheral representation in ventral than in dorsal visual areas.

In the annular wedge condition nearly all of the activity falls within a narrow range of phase corresponding to angular positions around the lower vertical meridian. Even portions of the brain that showed ordinary responses when presented with the full wedge responded at this abnormal phase in the annular wedge condition.

In addition, activation in response to the annular wedge can be observed just below the ventral boundary of V4v (Figure 4C). We have observed a representation of the lower visual quadrant in this region in the retinotopic flat maps of many of our normal subjects. Other fMRI studies have shown a representation of the lower visual quadrant in ventral cortex, claiming it as a part of V4 (McKeefry & Zeki, 1997) or part of an entirely new area, V8 (Hadjikhani et al., 1998). Again, these signals are consistent with the preservation of the lower vertical meridian representation in G.Y.

Responses in G.Y.'s intact occipital lobe were consistent with retinotopic measurements in the right occipital lobe of the normal observer (not shown). Signals in V1 were strongly driven by stimulus phases spanning 180 deg, representing the contralateral hemifield. Signals in dorsal and ventral extrastriate visual areas V2 and V3 were highly correlated with stimuli spanning 90 deg phase, corresponding to lower and upper quadrants of the visual field, respectively.

Phase Analyses

In this section, we provide a quantitative analysis of the data in order to determine more precisely which portions of the visual field are represented by the abnormal signals. The following figures show voxel frequency histograms as a function of angular position for different visual areas and for the two different rotating wedge conditions. Each histogram bar shows the number of voxels which exceeded the estimated noise level, a stimulus correlation of 0.2. Correlations of all the voxels in each angular position bin (including those below 0.2) were also averaged. The mean correlation was then calculated across all bins containing at least 20 voxels exceeding the 0.2 noise threshold.

The distribution of angular positions represented by voxels in each visual area in the lesioned occipital lobe is shown in Figure 5. Visual areas were identified using the response pattern to the full wedge stimulus (Figure 4A). The top row represents responses in the full wedge condition and the bottom row represents responses to the annular wedge.

In the lesioned occipital lobe, response phases were generally consistent with retinotopic representations of the visual field when G.Y. viewed the full wedge,

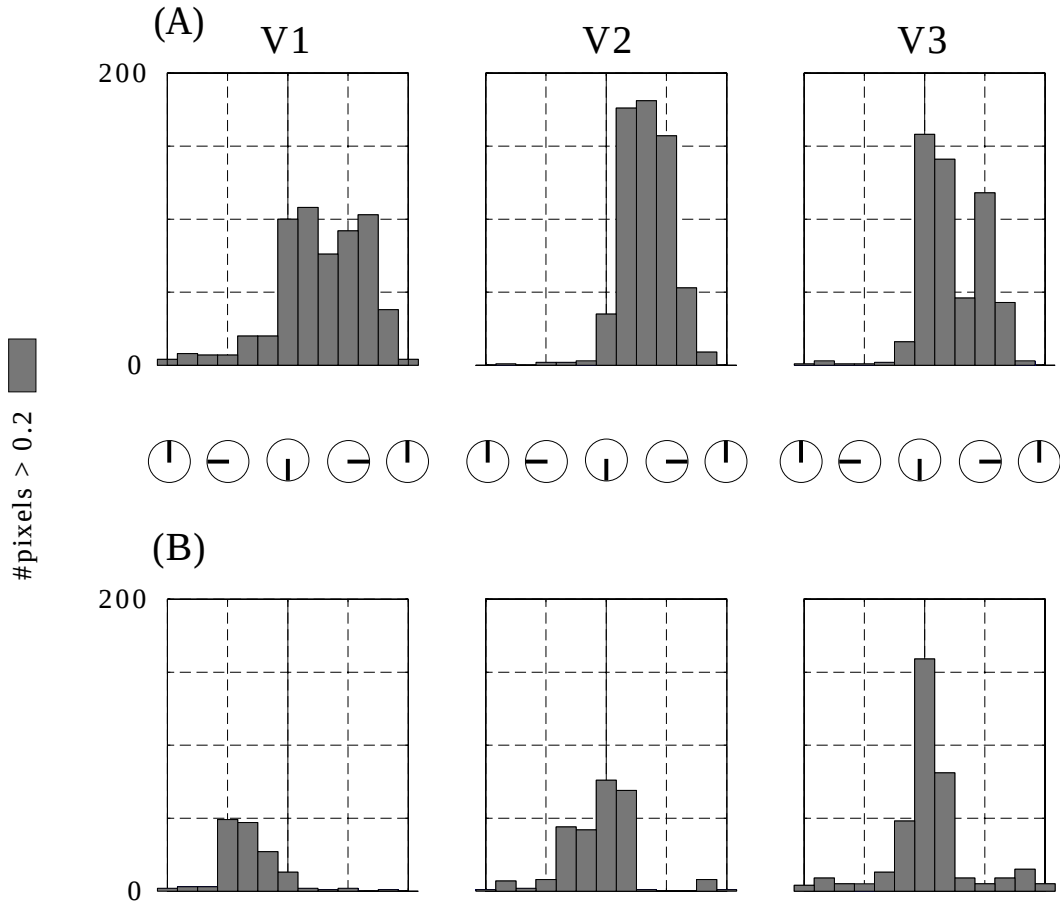

Figure 5: Summary of the fMRI responses within individual visual areas to the two types of rotating wedge stimulus in the left (damaged) occipital lobe. Each column summarizes responses from three different visual areas - V1, V2 and V3. Dorsal and ventral portions of V2 and V3 are combined here. The horizontal axis represents angular position of the visual field representation as inferred from the phase of the fMRI signal. The vertical axis indicates the number of voxels exceeding the 0.2 stimulus correlation level for each histogram bin. (A) Measurements using the full wedge stimulus. Mean correlations were: V1 = 0.33; V2 = 0.33; V3 = 0.33. (See text for explanation of mean correlation calculation). (B) Measurements using the annular wedge stimulus. Mean correlations were: V1 = 0.16; V2 = 0.22; V3 = 0.26.

although there were relatively few voxels responding to phases driven by visual field positions near the upper vertical meridian (Figure 5A).

The responses to the annular wedge, however, were quite different. Visual areas V1 and ventral regions of V2 and V3 displayed essentially no organized activity. Large signals were observed, however, in dorsal extrastriate visual areas V2 and V3 (also in V3a, not shown here). Hence, the clusters of responses around the lower vertical meridian in the pooled data (Figure 5B) are derived from dorsal and not ventral V2 and V3. The responses differ from normal controls in that (a) there is a reduced response to the horizontal meridian, and (b) the responses represent positions that extend into the ipsilateral hemifield across the lower vertical meridian.

Response positions represented in the visual areas in the left occipital lobe of the control subject, A.P., are shown for comparison in Figure 6. Note the similarity in the distributions between the two stimulus conditions (Figure 6A and B) in the normal subject.

Response positions represented in the visual areas of G.Y.'s right, non-lesioned occipital lobe are also shown in Figure 7. Although fewer voxels respond to the annular (B) than the full wedge stimulus (A), the distribution of angular positions represented is similar in the two conditions. In both conditions, responses in the right, intact, occipital lobe represent the contralateral, left hemifield.

Figure 8 shows histograms comparing activity in the full wedge and the annular wedge conditions in dorsal V2 and V3 with ventral V2 and V3. Both dorsal and ventral cortex respond to the appropriate visual field quadrants in the full wedge condition. However, only dorsal V2 and V3 respond to the annular wedge. Responses to the annular wedge were again confined to the vertical meridian representation. Dorsal and ventral areas in G.Y.'s intact, right occipital lobes, and in both occipital lobes of the control subject, A.P., responded to the appropriate contralateral quadrants for both wedge stimuli (not shown).

Comparison of annular and full wedge responses

The extrastriate activity caused by the annular wedge does not conform to conventional retinotopic positions (see Figure 4). Figure 9 shows the nature of the abnormal signals by making a direct comparison between the full and annular wedge responses. Each point represents the angular visual field representation of a single voxel that was active in both the full wedge and annular wedge experiments.

In the control subject, the angular representation is the same in the two stimulus conditions (Figure 9, A and B). The points fall close to a line with unit slope.

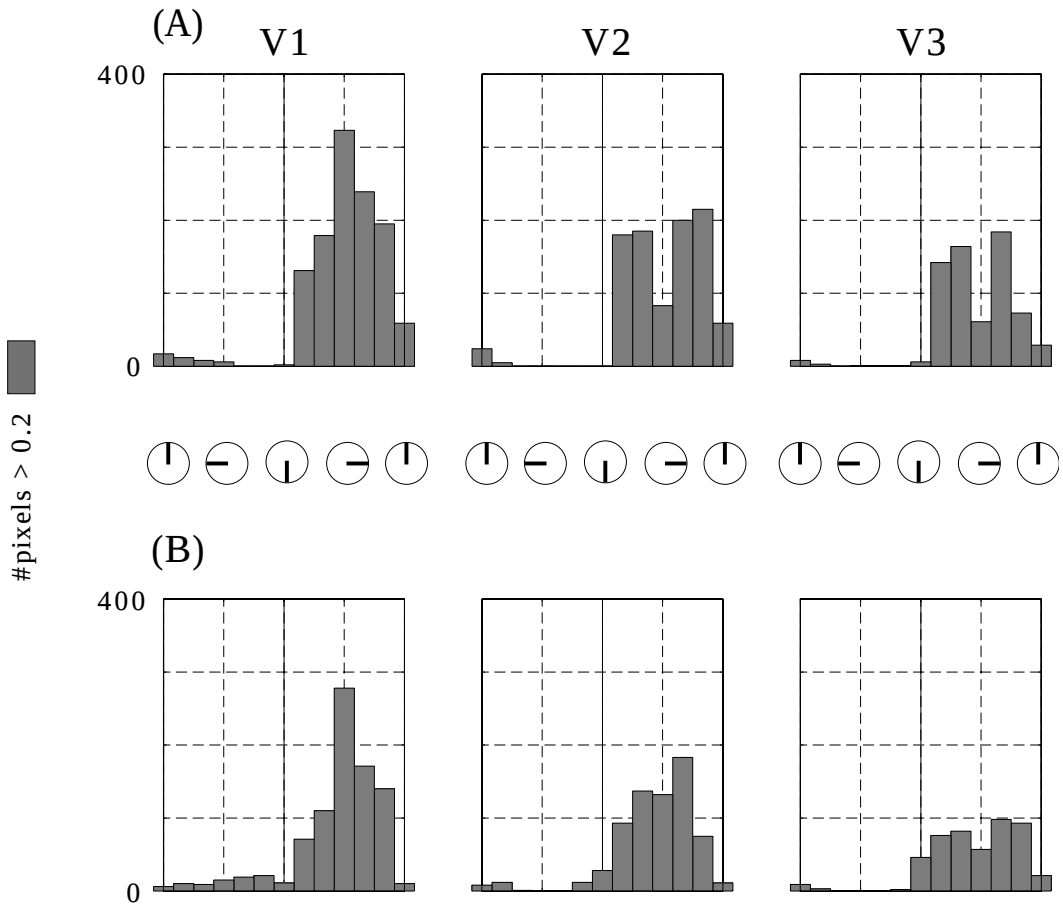

Figure 6: Summary of the fMRI responses within individual visual areas to the two types of rotating wedge stimulus in the left occipital lobe of the control subject, A.P. Details are as in Figure 5. (A) Measurements using the full wedge stimulus. Mean correlations were: V1 = 0.52; V2 = 0.46; V3 = 0.45. (B) Measurements using the annular wedge stimulus. Mean correlations were: V1 = 0.30; V2 = 0.38; V3 = 0.31.

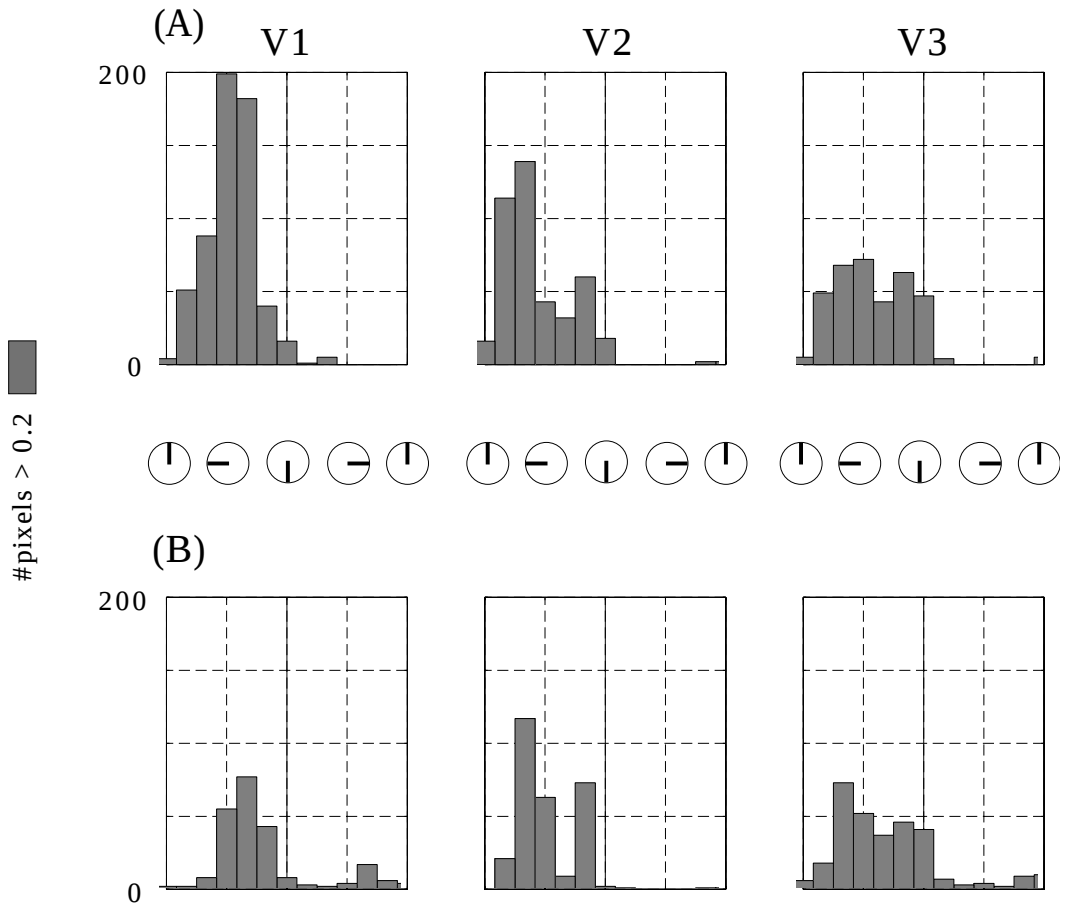

Figure 7: Summary of the fMRI responses within individual visual areas to the two types of rotating wedge stimulus in the non-lesioned, right occipital lobe of G.Y. Details are as in Figure 5. (A) Measurements using the full wedge stimulus. Mean correlations were: V1 = 0.35; V2 = 0.38; V3 = 0.36. (B) Measurements using the annular wedge stimulus. Mean correlations were: V1 = 0.22; V2 = 0.29; V3 = 0.29.

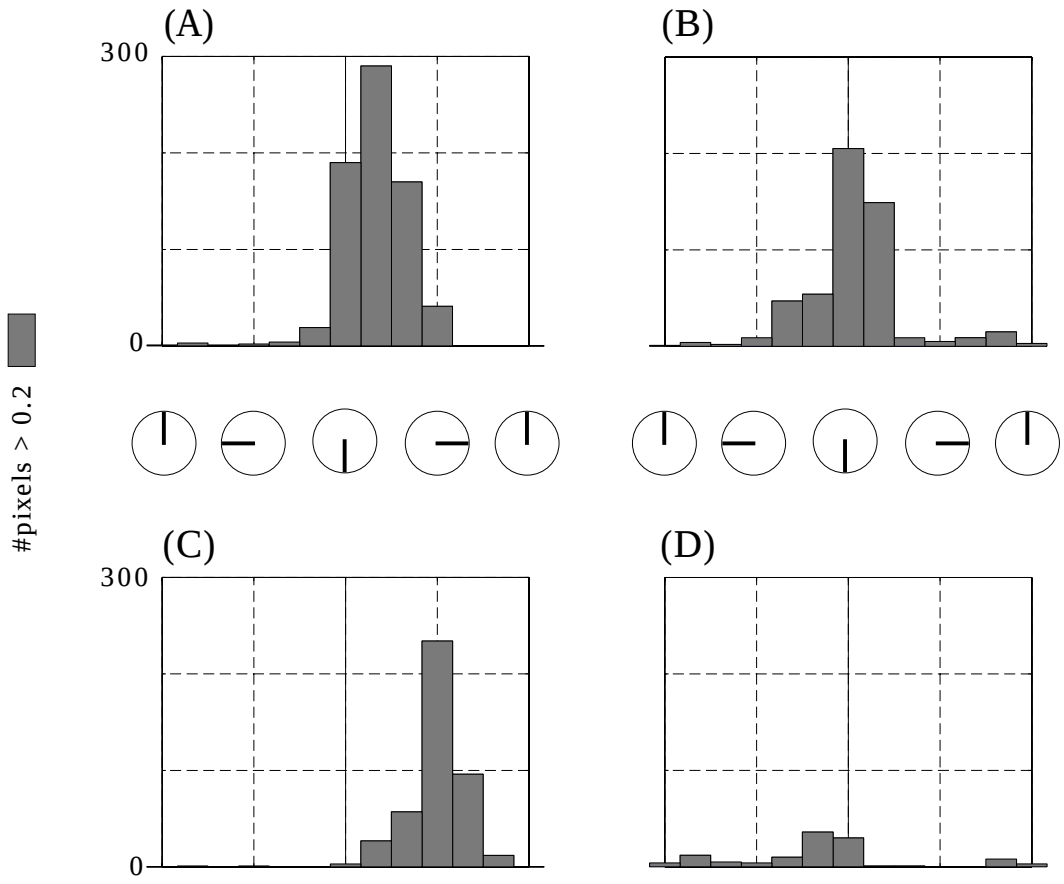

Figure 8: Comparison of the fMRI responses within dorsal and ventral areas to the two types of rotating wedge stimulus in G.Y.'s left (lesioned) occipital lobe. Responses from areas V2 and V3 are combined in each histogram. (A) Dorsal responses, full wedge stimulus. (B) Dorsal responses, annular wedge stimulus. (C) Ventral responses, full wedge stimulus. (D) Ventral responses, annular wedge stimulus. Other features as in Figure 5

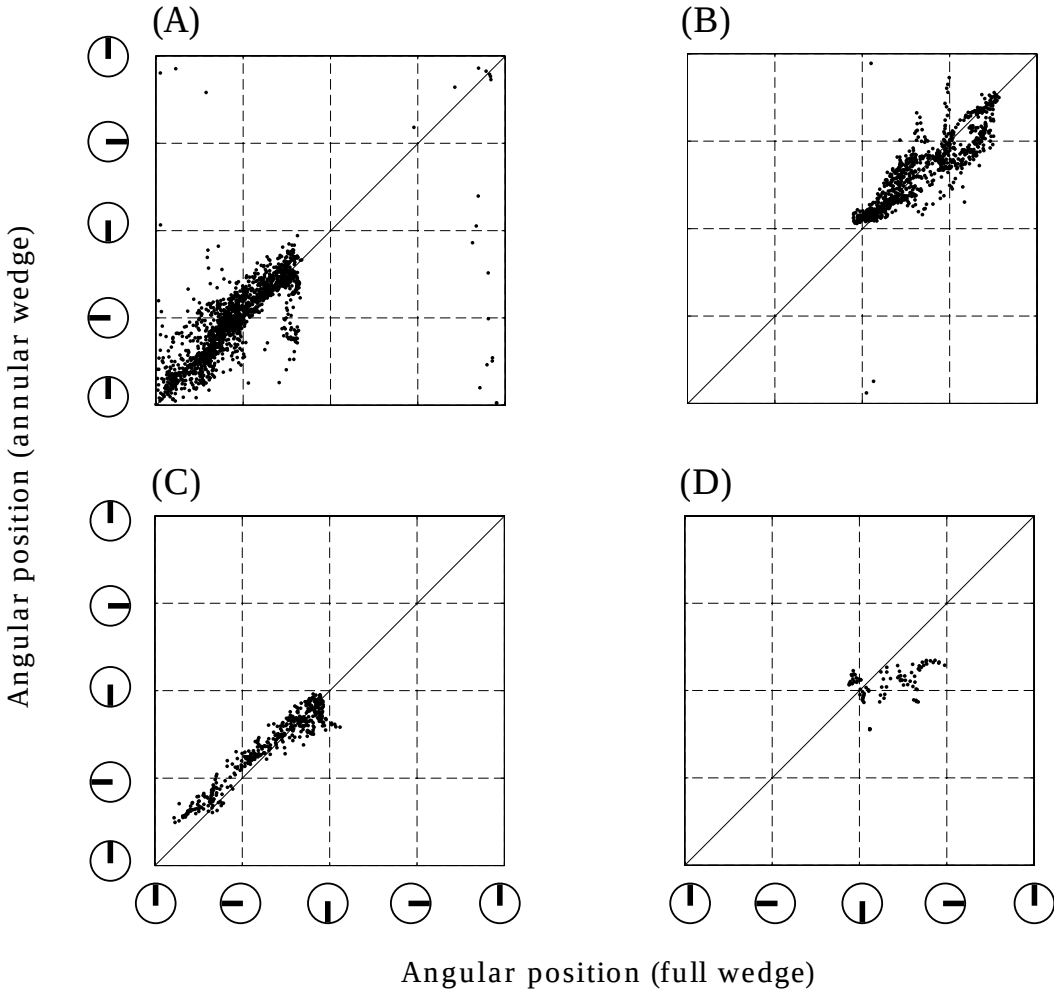

Figure 9: Comparison of angular visual field representation measured in the full (horizontal axis) and annular (vertical axis) wedge conditions. Voxels exceeding a correlation threshold of 0.33 in both stimulus conditions are shown. Responses from V1, V2 and V3, dorsal and ventral, V3a and V4v are pooled in each graph. The identity line is plotted for comparison. Because of the cyclic nature of the angular dimension, points falling at the far right (upper) margin of the graph also could be plotted at the far left (lower) margin. (A) Control subject A.P., right hemisphere; (B) Control subject A.P., left hemisphere; (C) G.Y., right hemisphere; (D) G.Y., left hemisphere.

Moreover, as expected, voxels in each occipital lobe represent an entire, contralateral hemifield. In G.Y.'s intact occipital lobe, the data are similar to the normal control (Figure 9C).

In G.Y.'s lesioned occipital lobe (Figure 9D) the angular representations in the two stimulus conditions differ. The collection of points falls significantly below the line of unit slope. The voxels active in both conditions are restricted to positions in the lower right quadrant, normally represented in the dorsal visual areas. The data show that the same region of cortex in G.Y.'s lesioned occipital lobe responds differently depending on the stimulus configuration. Hence, the annular wedge stimulus causes activity at cortical locations that are inconsistent with normal retinotopic organization.

Summary

We can summarize our measurements of the normal control, G.Y.'s intact occipital lobe, and G.Y.'s lesioned occipital lobe with the following points.

1. Stimulation within spared regions of the visual field produced normal retinotopic maps in the intact, right occipital lobe and in the intact, foveal representation of the lesioned, left occipital lobe. Several visual areas could be identified in both lobes, including V1, V2, V3, V3a and V4v.

2. The lesion in the left occipital lobe extends not only into the peripheral representation of V1, but also into the peripheral representations of ventral extrastriate areas V2v, V3v and V4v. Hence, stimulation restricted to the blind portion of the visual field generated activity within the lesioned occipital lobe primarily in dorsal extrastriate areas V2d, V3d and V3a.

3. Stimuli restricted to the blind portion of the visual field generated response patterns that were inconsistent with normal retinotopic organization. Extrastriate areas that had shown normal organization when the fovea was also stimulated, now responded primarily to positions near the lower vertical meridian.

Discussion

Related results

A prior neuroimaging (PET) study using moving stimuli in G.Y.'s blind field has demonstrated significant activation at several cortical positions (Barbur et al., 1993). Activity at the lateral junction of the occipital and parietal lobes (human MT+/V5) and also in area 7 were reported. In addition, an active location in the occipital lobe, thought to be V3, was observed. It has been suggested that the activity in MT+ may be caused by a direct projection from the dorsal LGN to MT+, though there is some disagreement on this point (ffytche et al., 1995; Hotson et al., 1994).

Human area MT+ is not retinotopically organized at the fMRI signal resolution. Consequently, the stimuli used in the present experiments did not produce significant activity in MT+. In separate experiments, however, we have confirmed the presence of significant activity in MT+ when G.Y. observed moving targets. Our acquisition planes did not extend anterior enough to measure activity in area 7.

The PET activations were obtained at a relatively coarse spatial resolution, but the reported activation of V3 in the superior occipital lobe was qualitatively in the position of dorsal V3 measured here. The region activated in the PET study extends to a position that is anterior to our measurement of of dorsal V3, but this can be explained in part by the fact that Barbur et al. used more eccentric stimuli (11 deg) than those used in this study. Contrary to our results, however, Barbur et al. (1993) generated activity in putative dorsal V3 with a stimulus that was restricted to the *upper* visual field. Dorsal V3 (V3d) in either hemisphere normally represents the *lower* visual quadrants. However, adjacent area V3a has been shown to contain both the upper and lower visual quadrants (Tootell et al., 1997).

Our measurements extend those of Barbur et al. in several ways. First, we have measured the location of several retinotopically organized visual areas. This has enabled us to unambiguously identify both the position of the lesion and residual neural responses with respect to functionally defined areas. Second, we have shown that residual activity is present in V2d, V3a and ventral to V4v in addition to V3. Third, we have provided more precise information about the representations of the visual field in the lesioned occipital lobe. Specifically, we have shown that the topography of extrastriate areas in G.Y. depends on the stimulus configuration.

Source of the blind hemifield signals

Next, we consider three possible sources of the signals we have measured in G.Y.'s lesioned occipital lobe.

First, in monkey, two subcortical pathways project directly to extrastriate visual areas. One pathway is from the pulvinar (via the superior colliculus) and a second is from the LGN. Anatomical studies in primate have shown that both the LGN (Fries, 1981; Yukie & Iwai, 1981; Bullier & Kennedy, 1983) and pulvinar projections (Kaas & Huerta, 1988) are sent to many areas of the extrastriate cortex. Following de-activation of V1 by cooling, single-unit measurements failed to find activity in V2,V3 and V4 but did find activity in area V3a (Girard et al., 1991a; Girard & Bullier, 1989; Girard et al., 1991a,b; Schiller & Malpeli, 1977). Because the direct projections from subcortical structures to extrastriate cortex are sparse, extrastriate activity may be difficult to detect during single-unit electrode recordings.

Direct subcortical projections have been proposed as the source of signals in residual vision (Weiskrantz et al., 1974; Barbur et al., 1980; Blythe et al., 1987; Barbur et al., 1993). However, because these subcortical structures are organized retinotopically and represent the entire visual field, it seems unlikely that they would generate activity in G.Y. only near the lower vertical meridian (Berson & Stein, 1995).

A spared strip of dorsal V1 beyond the macular representation is a second possible source for the signals in the lesioned occipital lobe. Barbur et al. (1993) also made a detailed perimetric map of G.Y.'s visual field (see Figure 2). In addition to the macular sparing, their map reveals a thin strip of spared vision in the right visual field along the lower vertical meridian. We were unaware of this observation until after our fMRI measurements were made, as it was not noted in the text or in other behavioral studies in G.Y. An earlier visual field map measured using static light stimuli failed to show a spared strip along the lower vertical meridian (Barbur et al., 1980). Note that the spared strip corresponds with the representation of residual activity in left, extrastriate cortex found in our data.

Our measurements do not support a residual V1 source for two reasons. First, there is only a fragmented and inconsistent response beyond the macular representation in the flattened representation (Figure 4). Second, the quantitative analyses of V1 using histograms show little V1 activity corresponding to the lower vertical meridian (Figure 5). Still, this region of V1 may contain a weak and spatially disorganized representation of the normal LGN signals that are difficult to detect using the phase-encoding methods.

Transcallosal fibers are a third possible source of the signals in the lesioned occipital lobe. In both monkey and human, the callosal fibers connecting early retinotopically

organized visual areas represent the vertical meridian (Zeki, 1970; Bunt & Minckler, 1977; Bunt et al., 1977; Van Essen et al., 1982; Clarke & Miklossy, 1990). Tootell et al. (1998) have confirmed the presence of ipsilateral activity, presumably mediated by callosal connections, in several retinotopically organized human visual areas. The activity in the lesioned occipital lobe, which is restricted to the lower vertical meridian, is consistent with a callosal source. The difference between the ventral and dorsal activity levels may be explained by the fact that the lesion lies somewhat ventral: dorsal fibers may be relatively spared. A psychophysical study in G.Y. has reported that he senses motion towards the vertical meridian in his blind visual field when moving stimuli are presented to his normal visual field (Finlay et al., 1997).

Cortical reorganization

Several recent reports have suggested a large range of plastic behavior within the human brain (e.g. Gilbert, 1996; Karni & Bertini, 1997; Gilbert, 1998; Buonomano & Merzenich, 1998). The highly detailed measurements we have obtained from G.Y.'s brain support the presence of plasticity in intact portions of the lesioned occipital lobe. Figure 4A shows that when foveal representations are activated, nearby peripheral representations in V2d and V3d exhibit normal angular topography. Figure 4C shows that when foveal stimulation is absent, the same regions in V2d and V3d now represent positions near the lower vertical meridian. These regions, which have been severed from their usual direct input, appear to be colonized by neighboring cortex that continues to receive input.

Figure 10 provides a framework for understanding how the same portion of cortex can respond differently in the full and annular wedge conditions. The data are explained assuming only changes in the relative significance of local connections. For simplicity, the figure shows only the signals in V1 and dorsal V2, although the same principle also applies to signals in dorsal V3.

In intact cortex, dorsal V2 receives its primary input from corresponding retinotopic representations in V1 (Figure 10A). In G.Y.'s lesioned occipital lobe, however, these inputs are absent. We assume that when V2 are deprived of their normal V1 input, they are colonized by other neurons in neighboring cortex (Figure 10B). The colonization may be mediated by strengthening or disinhibition of long-range connections or by the creation of new connections (Das & Gilbert, 1995). In the Figure, these new connections are indicated by the bold arrows.

The development of these new connections explains G.Y.'s measurements as follows. In the full wedge condition (Figure 4A) neurons representing the fovea drive the nearby peripheral representations and generate a normal representation of angular

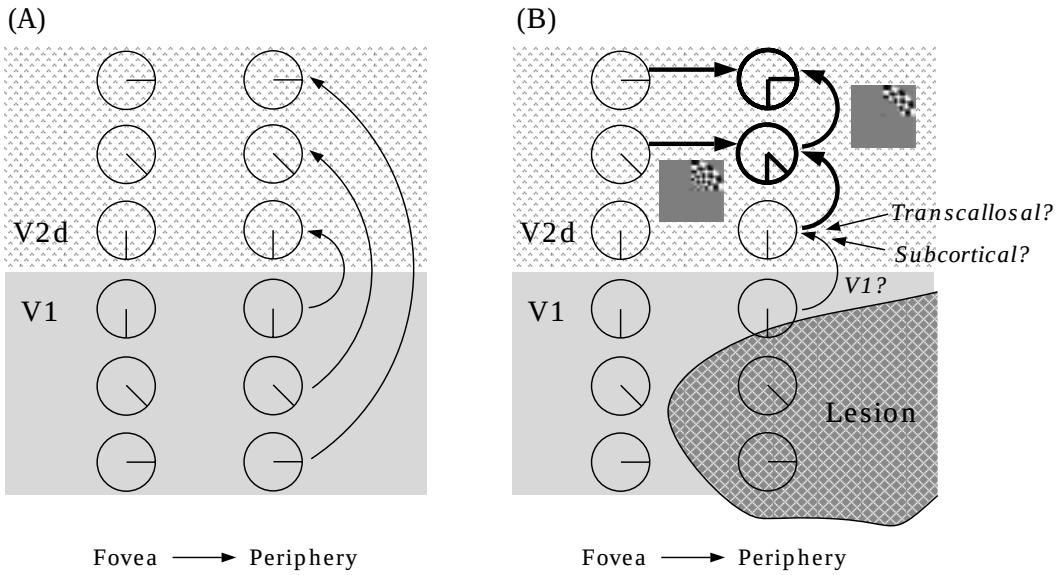

Figure 10: A framework for explaining G.Y.'s cortical responses. For simplicity, only the connectivity between V1 and V2d is illustrated. In both panels, the shaded gray region represents V1, and the lightly hatched area represents dorsal V2 (V2d). Circles with lines describe the angular representation at different cortical locations. The fovea is represented on the left and periphery to the right in each panel. (A) Intact occipital lobe. Primary, feed-forward inputs to V2d are shown as thin arrows. (B) Lesioned occipital lobe in G.Y. The lesion is indicated by the dark, hatched area. Altered inputs to V2d, possibly mediated by long-range horizontal connections, are represented by the bold arrows. The principal source of signals for either the full or annular wedge condition is identified by the stimulus icons.

visual field position. In the annular wedge condition, neurons representing the fovea are not stimulated. Instead, nearby neurons that represent the peripheral portion of the lower vertical meridian generate an abnormal representation of the visual field position (Figure 4C). Finally, when measured using an expanding ring stimulus, activity in the spared regions of V2d and V3d respond to both signals from the spared foveal signals and from the peripheral signals along the lower vertical meridian. This produces weak eccentric retinotopic organization (Figure 4B). That we do not see the same colonization of peripheral V2d and V3d in normal controls (Figure 3) suggests that the activity in G.Y. is mediated by connections that have been strengthened or added through plastic reorganization.

Our results demonstrate that human cortex reorganizes following lesions to primary sensory areas. The principles governing this reorganization can be understood based on simple recruitment of activity by nearby healthy cortex.

References

[1] J.L. Barbur and K.H. Ruddock. Spatial characteristics of movement detection mechanisms in human vision: I. achromatic vision. *Biol. Cybern.*, 37:77–92, 1980.

[2] J.L. Barbur, K.H. Ruddock, and V.A. Waterfield. Human visual responses in the absence of the geniculo-calcarine projection. *Brain*, 103:905–928, 1980.

[3] J.L. Barbur, J.D.G. Watson, R.S.J. Frackowiak, and S. Zeki. Conscious visual perception without V1. *Brain*, 116:1293–1302, 1993.

[4] D.M. Berson and J.J. Stein. Retinotopic organization of the superior colliculus in relation to the retinal distribution of afferent ganglion cells. *Visual Neuroscience*, 12:671–686, 1995.

[5] I.M. Blythe, C. Kennard, and K.H. Ruddock. Residual vision in patients with retrogeniculate lesions of the visual pathways. *Brain*, 110:887–905, 1987.

[6] G.M. Boynton, S.A. Engel, G.H. Glover, and D.J. Heeger. Linear systems analysis of functional magnetic resonance imaging in human V1. *J. Neuroscience*, 16:4207–4221, 1996.

[7] P.J. Brent, C. Kennard, and K.H. Ruddock. Residual colour vision in a human hemianope: spectral responses and colour discrimination. *Proc. R. Soc. Lond. B*, 256:219–225, 1994.

[8] J. Bullier and H. Kennedy. Projection of the lateral geniculate nucleus onto cortical area v2 in the macaque monkey. *Exp. Brain Res.*, 53:168–172, 1983.

[9] A.H. Bunt and D.S. Minckler. Foveal sparing. new anatomical evidence for bilateral representation of the central retina. *Archives of Ophthalmology*, 95:1445–1447, 1977.

[10] A.H. Bunt, D.S. Minckler, and G.W. Johanson. Demonstration of bilateral projection of the central retina of the monkey with horseradish peroxidase neuronography. *J. Comp. Neurol.*, 171:619–630, 1977.

[11] D.V. Buonomano and M.M. Merzenich. Cortical plasticity: from synapses to maps. *Annu. Rev. Neurosci.*, 21:149–186, 1998.

[12] G.G. Celesia, D. Bushnell, S.C. Toleikis, and M.G. Brigell. Cortical blindness and residual vision: Is the “second” visual system in humans capable of more than rudimentary visual perception? *Neurology*, 41:862–869, 1991.

[13] S. Clarke and J. Miklossy. Occipital cortex in man: Organization of callosal connections, related myelo- and cytoarchitecture, and putative boundaries of functional visual areas. *J. Comp. Neurol.*, 298:188–214, 1990.

[14] A. Das and C.D. Gilbert. Long-range horizontal connections and their role in cortical reorganization revealed by optical recording of cat primary visual cortex. *Nature*, 375:780–784, 1995.

[15] D.C. Van Essen, W.T. Newsome, and J.L. Bixby. The pattern of interhemispheric connections and its relationship to extrastriate visual areas in the macaque monkey. *J. Neuroscience*, 2:265–283, 1982.

[16] D.H. ffytche, C.N. Guy, and S. Zeki. Motion specific responses from a blind hemifield. *Brain*, 119:1971–1982, 1996.

[17] A.L. Finlay, S.R. Jones, A.B. Morland, J.A. Ogilvie, and K.H. Ruddock. Movement in the normal visual hemifield induces a percept in the "blind" hemifield of a human hemianope. *Proc. R. Soc. Lond.*, 264:267–275, 1997.

[18] W. Fries. The projection from the lateral geniculate nucleus to the prestriate cortex of the macaque monkey. *Proc. R. Soc. Lond. B*, 213:73–80, 1981.

[19] C. D. Gilbert. Adult cortical dynamics. *Physiol. Rev*, 78(2):467–485, 1998.

[20] C.D. Gilbert and T.N. Wiesel. Receptive field dynamics in adult primary visual cortex. *Nature*, 356:150–152, 1992.

[21] P. Girard and J. Bullier. Visual activity in area V2 during reversible inactivation of area 17 in the macaque monkey. *J. Neurophysiology*, 62:1287–1302, 1989.

[22] P. Girard, P.A. Salin, and J. Bullier. Visual activity in areas V3a and V3 during reversible inactivation of area V1 in the macaque monkey. *J. Neurophysiology*, 66:1493–1503, 1991.

[23] P. Girard, P.A. Salin, and J. Bullier. Visual activity in macaque area V4 depends on area 17 input. *NeuroReport*, 2:81–84, 1991.

[24] N. Hadjikhani, A.K. Liu, A.M. Dale, P. Cavanagh, and R.B.H. Tootell. Retinotopy and color sensitivity in human visual cortical area v8. *Nature Neuroscience*, 1:235–241, 1998.

[25] S.J. Heinen and A.A. Skavenski. Recovery of visual responses in foveal v1 neurons following bilateral foveal lesions in adult monkey. *Exp. Brain Res.*, 83:670–674, 1991.

[26] J. Hotson, D. Braun, W. Herzberg, and D. Boman. Transcranial magnetic stimulation of extrastriate cortex degrades human motion direction discrimination. *Vision Research*, 34:2115–2123, 1994.

[27] D.H. Hubel and T.N. Wiesel. The period of susceptibility to the physiological effects of unilateral eye closure in kittens. *J. Physiol.*, 206:419–436, 1970.

[28] J.H. Kaas and M.F. Huerta. The subcortical visual system of primates. In H.D. Steklis and J. Erwin, editors, *Comparative Primate Biology*, volume 4, pages 327–391. A.R. Liss, Inc., 1988.

[29] J.H. Kaas, L.A. Krubitzer, Y.M. Chino, A.L. Langston, E.H. Polley, and N. Blair. Reorganization of retinotopic cortical maps in adult mammals after lesions of the retina. *Science*, 248:229–231, 1990.

[30] R.W. Kentridge, C.A. Heywood, and L. Weiskrantz. Residual vision in multiple retinal locations within a scotoma: Implications for blindsight. *J. Cognitive Neuroscience*, 9:191–202, 1997.

[31] D.R. Lucas, H.A. Baseler, and S.J. Heinen. Eye movements during extended fixation of a stationary target. *Invest. Ophthalmol. Vis. Sci.*, 37:S717, 1996.

[32] D.J. McKeefry and S. Zeki. The position and topography of the human colour centre as revealed by functional magnetic resonance imaging. *Brain*, 120:2229–2242, 1997.

[33] C.H. Meyer, B.S. Hu, D.G. Nishimura, and A. Macovski. Fast spiral coronary artery imaging. *Mag. Res. Med*, 28:202–213, 1992.

[34] A.B. Morland, J.A. Ogilvie, K.H. Ruddock, and J.R. Wright. Orientation discrimination is impaired i the absence of the striate cortical contribution to human vision. *Proc. R. Soc. Lond. B*, 263:633–640, 1996.

[35] S. Ogawa, T.M. Lee, A.R. Kay, and D.W. Tank. Brain magnetic resonance imaging with contrast dependent on blood oxygenation. *Proc. Natl. Acad. Sci. USA*, 87:9868–9872, 1990.

[36] M.T. Perenin. Discrimination of motion direction in perimetrically blind fields. *Neuroreport*, 2:397–400, 1991.

[37] H.R. Rodman, C.G. Gross, and T.D. Albright. Afferent basis of visual response properties in area MT of the macaque. i. effects of striate cortex removal. *J. Neuroscience*, 9:2033–2050, 1989.

[38] P.H. Schiller and J.G. Malpeli. The effect of striate cortex cooling on area 18 cells in the monkey. *Brain Research*, 126:366–369, 1977.

[39] C.J. Shatz. Emergence of order in visual system development. *Proc. Natl. Acad. Sci. USA*, 93:602–608, 1996.

[40] A.T. Smith, M.W. Greenlee, K.D. Singh, F.M. Kraemer, and J. Hennig. The processing of first- and second-order motion in human visual cortex assessed by functional magnetic resonance imaging (fmri). *J. Neuroscience*, 18:3816–3830, 1998.

[41] G.P. Standage and L.A. Benevento. The organization of connections between the pulvinar and visual area MT in the macaque monkey. *Brain Research*, 262:288–294, 1983.

[42] P. Teo, G. Sapiro, and B.A. Wandell. Creating connected representations of cortical gray matter for functional MRI visualization. *IEEE Med. Trans.*, 16:852–863, 1997.

[43] R.B.H. Tootell, J.D. Mendola, N.K. Hadjikhani, P.J. Ledden, A.K. Liu, J.B. Reppas, M.I. Sereno, and A.M. Dale. Functional analysis of v3a and related areas in human visual cortex. *J. Neuroscience*, 17:7060–7078, 1997.

[44] R.B.H. Tootell, J.D. Mendola, N.K. Hadjikhani, A.K. Liu, and A.M. Dale. The representation of the ipsilateral visual field in human cerebral cortex. *Proc. Natl. Acad. Sci. USA*, 95:818–824, 1998.

[45] L. Weiskrantz, J.L. Barbur, and A. Sahraie. Parameters affecting conscious versus unconscious visual discrimination with damage to the visual cortex (V1). *Proc. Natl. Acad. Sci. USA*, 92:6122–6126, 1995.

[46] L. Weiskrantz, E.K. Warrington, M.D. Sanders, and J. Marshall. Visual capacity in the hemianopic field following a restricted occipital ablation. *Brain*, 97:709–728, 1974.

[47] M. Yukie and E. Iwai. Direct projection from the dorsal lateral geniculate nucleus to the prestriate cortex in macaque monkeys. *J. Comp. Neurol.*, 201:81–97, 1981.

[48] S.M. Zeki. Interhemispheric connections of prestriate cortex in monkey. *Brain Research*, 19:63–75, 1970.